Copyright © 2010 Tech Science Press CMC, vol.16, no.2, pp.175-194, 2010

Lattice Dynamics and Second and Third Order Elastic Constants of Iron at Elevated Pressures

Hieu H. Pham[1] **and Tahir Çağın**[1]

Abstract: We analyze the lattice dynamics of Fe in different crystal phases (bcc, fcc and hcp) by using density-functional theory. The study on equations of states indicates that bcc Fe is more stable than fcc and hcp Fe at low pressures. However, dynamical instabilities in lattice vibrations of bcc Fe predict a phase transformation from bcc to hcp at higher pressures. We reported a complete set of second-order and third-order elastic constants of Fe in these three phases. We observed a linear variation in the values of second order elastic constant as a function of increased pressures. The phonon spectra were also analyzed to understand the stability of Fe in different phases.

Keywords: Iron, Elasticity, Phase behavior, Phonon instability, First Principles.

1 Introduction

Understanding the mechanical properties of iron under high pressure and large anisotropic loads is essential in order to interpret its behavior beyond elastic response regime. When dealing with infinitesimal strains, elasticity is fundamental for any solid materials. Broadly speaking, it is related to the internal energy and binding forces [Hull and Bacon (2001)], as the elastic resistance of a substance emerges as its response to applied loads through repulsive and attractive forces between atoms. Elastic coefficients may be important quantities to interpret the structural stability and phase transformations in crystals [Lew, Caspersen, Carter and Ortiz (2006)]. In general, the second-order elastic constants (SOEC) describe the response of materials to the linear deformation, whereas the third- and higher-order elastic constants (TOEC and HOEC) correspond to non-linear elasticity [Hiki (1981)]. Also, elasticity is essential in evaluating various mechanical and thermal properties, such as equation of state, pressure derivative of elastic constants [Çağın and Pettitt (1989)], thermal expansion, phonon-phonon interaction [Hiki

[1] Artie McFerrin Department of Chemical Engineering, Texas A&M University, College Station, TX, U.S.A.

(1981)], and acoustic amplification of microwave frequencies [Graham (1972)]. Particularly, studying the elasticity of hexagonal close-packed (hcp) iron is critical in explaining the elastic anisotropy, seismic behavior and differential rotation of the Earth's interior since hcp is the stable form at high pressures [Song and Richards (1996; Steinle-Neumann, Stixrude, Cohen and Gulseren (2001; Stixrude and Cohen (1995; 1995)].

The measurements of elastic coefficients can be conducted by various experimental techniques. Ultrasonic measurements [Fritz and Graham (1974)] or shock compression experiments [Graham (1972)] are used to obtain SOEC. TOEC can be experimentally measured through the determination of the change in the acoustic velocities under hydrostatic and uniaxial stresses [Brugger (1964); Nakagawa, Yamanouc.K and Shibayam.K (1973)]. The forth-order elastic constants (FOEC) could also be determined by using shock-compression methods [Graham (1972)]. However, due to the difficulties in these works, the experimental measurements on TOEC or HOEC require that many of efforts be made [Graham (1972; Johal and Dunstan (2006)], especially for those under extreme conditions. Due to advances in computational techniques and computer resources, several theoretical approaches are now available to calculate these quantities, including molecular dynamics [Çağın and Pettitt (1989); Çağın and Ray (1988); Çağın, Karasawa, Dasgupta and Goddard (1992); Çağın (1993); Çağın, Kimura, Qi, Ikeda, Johnson and Goddard(1999)] and first-principle methods [Lopuszynski and Majewski (2007); Nielsen (1986); Zhao, Winey and Gupta (2007); Uludogan, Çağın, (2006); Uludogan, Guarin, Gomez, Çağın, Goddard, (2008); Kart, Uludogan, Karaman, Çağın, (2008); Bilge, Kart, Kart, Çağın (2008); Chakrabarty, Çağın, (2008); Kalay, Kart, Kart, Çağın, (2009); Sevik, Çağın, (2009); Ojeda, Çağın, (2010)].

In this paper, we describe a method for determining SOEC and TOEC from strain-energy and applied strain relationships. In addition, we present associated first-principles calculations for SOEC and TOEC of iron using the Density Functional Theory (DFT) [Kohn and Sham (1965)], which is implemented in Vienna Ab initio Simulation Package (VASP) [Kresse and Furthmuller (1996)]. We use the Projector-Augmented Wave (PAW) methods [Bl ochl (1994)] to simulate the magnetic and crystal properties of iron. The PBE Generalized Gradient Approximation (GGA) exchange-correlation [Perdew, Burke and Ernzerhof (1996)] is employed. The spin-polarized calculations are adopted to simulate the magnetic phase. In the k-point sampling, we use a 16 x 16 x 16 Monkhorst-Pack grid [Monkhorst and Pack (1976)] for the plane wave basis in bcc and fcc Fe unit cells, and 20 x 20 x 20 grid for hcp cell, respectively. A cut-off energy at 440 eV was used for all simulations, which in turn yields a convergence of total energy within 1 meV/atom.

The organization of the paper is as follows. In section 2, we review the basics on

theory of elasticity and the calculation methods employed to elastic constants. In section 3, we report and discuss our results on iron equation of state (EOS), elastic constants, phonon spectra and phase stability of various crystal forms of Iron. The conclusion will be delivered in the last section.

2 Theoretical approach

The relationship between strain energy, elastic constants and strains can be described in terms of the elasticity theory () [Murnaghan (1967)]. For a crystal domain, **X= (I+** ε**)A** is the deformed lattice under the application of a strain matrix ε to the initial lattice vectors **A** (where **I** is the 3 x 3 unit matrix). Also, the transformation from a certain point A (a_1, a_2, a_3) in initial unstrained domain, into X (x_1, x_2, x_3 in deformed domain, is characterized by a Jacobian matrix **J**:

$$J_{ij} = \frac{\partial x_j}{\partial a_i} \tag{1}$$

The symmetric Lagrangian strain parameters ε_{ij} are then given as [Wallace (1972)]

$$\varepsilon_{ij} = \frac{1}{2}\sum_{n=1}^{3}\left(\frac{\partial x_n^2}{\partial a_i \partial a_j} - \delta_{ij}\right) \text{ or } \varepsilon = \frac{1}{2}(J^T J - I) \tag{2}$$

Where δ_{ij} is the Kronecker delta.The densities in the initial undeformed and final deformed state, (ρ_0 and ρ respectively), are related to each other through the determinant of the Jacobian ($\rho_0 = \rho$ det **J);** therefore the strain matrix, ε**,** yields a volume-conserving deformation in case of a unit-determinant J [Mehl, Osburn, Papaconstantopoulos and Klein (1990)]. Since deformation tensors are symmetric, we use the Voigt index notation for convenience: (11) → 1, (22) → 2, (33) → 3, (23) → 4, (13) → 5, (12) → 6. Thus, a 3 x 3 symmetric strain matrix,ε**,** can be simplified to a 6-dimensional vector η:

$$\varepsilon = \begin{pmatrix} \varepsilon_{11} & \varepsilon_{12} & \varepsilon_{13} \\ \varepsilon_{21} & \varepsilon_{22} & \varepsilon_{23} \\ \varepsilon_{31} & \varepsilon_{32} & \varepsilon_{33} \end{pmatrix} = \begin{pmatrix} \eta_1 & \frac{1}{2}\eta_6 & \frac{1}{2}\eta_5 \\ \frac{1}{2}\eta_6 & \eta_2 & \frac{1}{2}\eta_4 \\ \frac{1}{2}\eta_5 & \frac{1}{2}\eta_4 & \eta_3 \end{pmatrix} \vec{\eta} = \begin{pmatrix} \eta_1 \\ \eta_2 \\ \eta_3 \\ \eta_4 \\ \eta_5 \\ \eta_6 \end{pmatrix} = \begin{pmatrix} \varepsilon_{11} \\ \varepsilon_{22} \\ \varepsilon_{33} \\ \varepsilon_{23} + \varepsilon_{32} \\ \varepsilon_{13} + \varepsilon_{31} \\ \varepsilon_{12} + \varepsilon_{21} \end{pmatrix} = \begin{pmatrix} \varepsilon_{11} \\ \varepsilon_{22} \\ \varepsilon_{33} \\ 2\varepsilon_{23} \\ 2\varepsilon_{13} \\ 2\varepsilon_{12} \end{pmatrix} \tag{3}$$

Stress components $\sigma_{\alpha\beta}$ (α, β =1, 2, 3 in Cartesian coordinates) are defined as the force in α^{th}axis on the plane with outward normal in β^{th} direction. The generalized

Hooke's law [Nye (1957)] gives the relation between the stress, elastic modulus and strain: $\sigma_{\alpha\beta} = C_{\alpha\beta\mu\nu}\eta_{\mu\nu}$ or, $\sigma_I = C_{IJ}\eta_J$ in Voigt notation.

In addition, the thermodynamic definition of adiabatic (constant S) and isothermal (constant T) n-order elastic constants given by Brugger are widely used [Brugger (1964; Wallace (1972)]:

$$C^S_{ijkl..mn} = \rho_0\left(\frac{\partial^n U}{\partial\varepsilon_{ij}\partial\varepsilon_{kl}\cdots\partial\varepsilon_{mn}}\right)_S \tag{4}$$

where U and F are internal energy and free energy, respectively and ρ_0 is the specific density of the unstrained medium.

In this paper, total energy was calculated by DFT at 0 K; therefore elastic constants can be referred to as isothermal. The tensor stress is described by following equation:

$$\sigma_{\alpha\beta} = \frac{\rho}{\rho_0}\sum_{m,n=1}^{3}\frac{\partial x_\alpha}{\partial a_m}\frac{\partial U}{\partial\varepsilon_{mn}}\frac{\partial x_\beta}{\partial a_n} \tag{5}$$

The elastic energy per crystal unit volume upon application of a Lagrangian strain tensor, η, may be expanded in terms of elastic constants as the expansion coefficients [Brugger (1964)]:

$$\rho_0\Delta F(\eta) = \frac{1}{2!}\sum_{IJ=1\cdots6} C_{IJ}\eta_I\eta_J + \frac{1}{3!}\sum_{IJK=1\cdots6} C_{IJK}\eta_I\eta_J\eta_K + \Theta(\eta^4) \tag{6}$$

Due to high symmetry in the stress and strain tensors of a cubic crystal, a fourth-rank SOEC tensor can be reduced to a 6 x 6 symmetric matrix with only 12 non-zero SOEC terms, and three of them are independent (C_{11}, C_{12} and C_{44}). Therefore the general form of second-order term in equation (6) can be derived for a cubic crystal as follows.

$$\sum_{IJ=1\cdots6} C_{IJ}\eta_I\eta_J = (\eta_1,\eta_2,\eta_3,\eta_4,\eta_5,\eta_6,). \begin{pmatrix} C_{11} & C_{12} & C_{12} & 0 & 0 & 0 \\ C_{12} & C_{11} & C_{12} & 0 & 0 & 0 \\ C_{12} & C_{12} & C_{11} & 0 & 0 & 0 \\ 0 & 0 & 0 & C_{44} & 0 & 0 \\ 0 & 0 & 0 & 0 & C_{44} & 0 \\ 0 & 0 & 0 & 0 & 0 & C_{44} \end{pmatrix} \cdot \begin{pmatrix} \eta_1 \\ \eta_2 \\ \eta_3 \\ \eta_4 \\ \eta_5 \\ \eta_6 \end{pmatrix}$$

$$
\begin{aligned}
&= C_{11}(\eta_1^2+\eta_2^2+\eta_3^2)+2C_{12}(\eta_1\eta_2+\eta_2\eta_3+\eta_3\eta_1)+C_{44}(\eta_4^2+\eta_5^2+\eta_6^2)\\
\text{or} &= C_{11}(\varepsilon_{11}^2+\varepsilon_{22}^2+\varepsilon_{33}^2)+2C_{12}(\varepsilon_{11}\varepsilon_{22}+\varepsilon_{22}\varepsilon_{33}+\varepsilon_{33}\varepsilon_{11})+4C_{44}(\varepsilon_{23}^2+\varepsilon_{13}^2+\varepsilon_{12}^2)
\end{aligned}
\tag{7}
$$

Under the uniaxial strain (i.e η_i=0 for i $\neq$ 1), this expression will remain the only contribution from C_{11}. The biaxial strain (η_i=0 for i $\neq$ 1, 2) contribution is given in terms of C_{11} and C_{12}; likewise, a strain tensor with zero diagonal components leads to a contribution of C_{44} alone. Hence, choices of strain tensors will result in a system of linear equations on elastic constants as variables.

The symmetry analysis leads to 6 distinct TOEC for cubic crystals [Fumi (1951)]; and the expansion of the third-order term in equation (6) yields the following combination of cubic crystal TOEC:

$$
\begin{aligned}
&\sum_{I,J,K=1\cdots6} C_{IJK}\eta_I\eta_J\eta_K =\\
&C_{111}(\eta_1^2+\eta_2^2+\eta_3^2)+3C_{112}(\eta_1^2\eta_2+\eta_2^2\eta_1+\eta_2^2\eta_3+\eta_3^2\eta_2+\eta_3^2\eta_1+\eta_1^2\eta_3)\\
&+6C_{123}\eta_1\eta_2\eta_3+3C_{144}(\eta_1\eta_4^2+\eta_2\eta_5^2+\eta_3\eta_6^2)\\
&+3C_{155}(\eta_2\eta_4^2+\eta_3\eta_4^2+\eta_1\eta_5^2+\eta_3\eta_5^2+\eta_1\eta_6^2+\eta_2\eta_6^2)\\
&+6C_{456}\eta_4\eta_5\eta_6
\end{aligned}
\tag{8}
$$

Low symmetrical crystals have more distinct elastic constants than high symmetrical crystals. Specifically, the hcp crystals have 5 independent SOEC, and the 2-order term in equation (6) for an hcp crystal can be given as follows:

$$
\begin{aligned}
&\sum_{IJ=1\cdots6} C_{IJ}\eta_I\eta_J\\
&= (\eta_1,\eta_2,\eta_3,\eta_4,\eta_5,\eta_6,).\begin{pmatrix} C_{11} & C_{12} & C_{13} & 0 & 0 & 0\\ C_{12} & C_{11} & C_{13} & 0 & 0 & 0\\ C_{13} & C_{13} & C_{33} & 0 & 0 & 0\\ 0 & 0 & 0 & C_{44} & 0 & 0\\ 0 & 0 & 0 & 0 & C_{44} & 0\\ 0 & 0 & 0 & 0 & 0 & (C_{11}-C_{12})/2 \end{pmatrix}\cdot\begin{pmatrix}\eta_1\\ \eta_2\\ \eta_3\\ \eta_4\\ \eta_5\\ \eta_6\end{pmatrix}\\
&= C_{11}(\eta_1^2+\eta_2^2+\frac{1}{2}\eta_6^2)+C_{12}(2\eta_1\eta_2-\frac{1}{2}\eta_6^2)+2C_{13}(\eta_1\eta_3+\eta_2\eta_3)\\
&\quad +C_{33}\eta_3^2+C_{44}(\eta_4^2+\eta_5^2)
\end{aligned}
\tag{9}
$$

For completeness, the expression below is derived for contribution to strain energy from TOEC in the hcp phase, using the symmetry table given by Fumi [Fumi

(1952)]:

$$\sum_{IJK=1\cdots6} C_{IJK}\eta_I\eta_J\eta_k =$$
$$C_{111}(\eta_1^3+3\eta_1\eta_2^2-\frac{3}{2}\eta_1\eta_6^2+\frac{3}{2}\eta_2\eta_6^2)$$
$$+C_{112}(3\eta_1^2\eta_2+3\eta_1\eta_2^2-\frac{3}{4}\eta_1\eta_6^2-\frac{3}{4}\eta_2\eta_6^2)$$
$$+C_{113}(3\eta_1^2\eta_3+3\eta_2^2\eta_3+\frac{3}{2}\eta_3\eta_6^2)+C_{114}(3\eta_1^2\eta_4+3\eta_1\eta_5\eta_6-3\eta_2^2\eta_4+3\eta_2\eta_5\eta_6)$$
$$+C_{123}(6\eta_1\eta_2\eta_3-\frac{3}{2}\eta_3\eta_6^2)$$
$$+C_{124}(6\eta_1\eta_2\eta_4+9\eta_1\eta_5\eta_6-6\eta_2^2\eta_4-3\eta_2\eta_5\eta_6+3\eta_4\eta_6^2)$$
$$+C_{133}(3\eta_1\eta_3^2+3\eta_2\eta_3^2)+C_{134}(6\eta_1\eta_3\eta_4-6\eta_2\eta_3\eta_4+6\eta_3\eta_5\eta_6)$$
$$+C_{144}(3\eta_1\eta_4^2+3\eta_2\eta_5^2-3\eta_4\eta_5\eta_6)$$
$$+C_{155}(3\eta_1\eta_5^2+3\eta_2\eta_4^2+3\eta_4\eta_5\eta_6)+C_{222}(-3\eta_1\eta_2^2+\frac{9}{4}\eta_1\eta_6^2+\eta_2^3-\frac{3}{4}\eta_2\eta_6^2)$$
$$+C_{333}(\eta_3^3)+C_{344}(3\eta_3\eta_4^2+3\eta_3\eta_5^2)+C_{444}(\eta_4^3-3\eta_4\eta_5^2) \tag{10}$$

Due to the sensitivity of elastic constants calculations, especially TOEC, to the maximum value of strains, the strains in this work are applied within the range of -0.035 to +0.035.

3 Results and Discussions

3.1 Equations of State (EoS)

Depending on external conditions, iron is observed to have various phases, including body-centered cubic (bcc), face-centered cubic (fcc), and hexagonal close-packed (hcp) [Yoo, Akella, Campbell, Mao and Hemley (1995)]. Crystal structure of ground-state iron is ferromagnetic bcc with 2 atoms contained in a conventional cubic unit cell. Upon increased pressure and temperature, iron undergoes phase transformations into close-packed structures: fcc and hcp. The hcp iron was reported to be the stable phase at the Earth's interior conditions [Jephcoat and Olson (1987; Laio, Bernard, Chiarotti, Scandolo and Tosatti (2000)]. In addition, the transition of iron from bcc to hcp begins around 9-13 GPa [Lew, Caspersen, Carter and Ortiz (2006)], and the transformation to fcc occurs at 1150 K [Sha and Cohen (2006)]

In this work, the equilibrium state of iron is determined by studying the behavior

of energy and pressure, i.e., the EoS for bcc, fcc, and hcp Fe at 0 K. The atomic energy curves are displayed for different structures in Fig. 1, in which bcc Fe is considered as ferromagnetic, and fcc and hcp are both of non-magnetic phases. In fact, our calculations show that the magnetic field yields no change in total energy of fcc and hcp crystals, which in turn confirms about no magnetization contribution in those phases. From the plot, the bcc crystal is more stable at 0 K condition and possesses a smaller atomic packing factor (APF). This observation is consistent with theoretical calculations, in which bcc crystal has an APF of 0.64 vs. 0.74 for fcc and hcp. If far from the zero pressure, the hcp phase could be more favorable than the bcc and that critical point could be around 70 GPa (Fig. 2). In this work, we focus on bcc and hcp structures, since they are naturally observed crystalline phases of Fe.

Based on the EoS plots, the equilibrium lattice parameter can be determined as the point of minimum energy and hence the zero pressure. The visual inspection gives a value approximately at two-thirds the distance between 2.80 and 2.85 Å for bcc iron. However, the zero-pressure lattice parameter, bulk modulus and its pressure derivative can also be obtained by fitting the data to an EoS expression for metals. We used the E-V and P-V relations introduced by [Li, Liang, Guo and Liu (2005)], which was a modified version of the Vinet and Rose equation [Vinet, Ferrante, Rose and Smith (1987)].

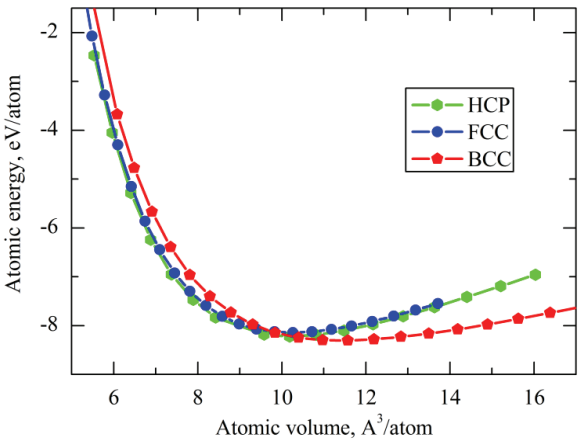

Figure 1: Variation of atomic energy as a function of atomic volume in Fe bcc, fcc and hcp phases

The EoS results show a good agreement with the experimental and previous theoretical calculations (Tab. 1). The theoretical lattice parameter calculated using DFT

Table 1: Equation of State parameters of bcc, fcc, hcp Fe a: [Jephcoat, Mao and Bell (1986)]; b: [Jiang and Carter (2003)]; c: [Lew, Caspersen, Carter and Ortiz (2006)]

Fe polymorphs	Methods	Atomic volume $Å^3$/ (lattice constant, Å)	Bulk modulus B_0, GPa	First pressure derivative B_0'
BCC Fe	Theory, bcc Fe	11.44 (/ 2.839)	177.9	5.09
	Expt., bcc Fe [a]	11.78 (/ 2.866)	172	5.0
	Comp. ref., bcc Fe [b]	11.33 (/ 2.83)	174	–
FCC Fe	Theory, fcc Fe	10.24 (/ 3.447)	285.4	4.70
	Comp. ref., fcc Fe [b]	10.27(/3.45)	282	–
HCP Fe	Theory, hcp Fe	10.18	290.3	4.71
	Expt., hcp Fe [c]	11.2	208	–
	Comp. ref., hcp Fe [c]	10.26	288	–

tends to be slightly below that of experimental measurements. In addition, our theoretical calculation on hcp bulk modulus, as well as the report by [Lew, Caspersen, Carter and Ortiz (2006)], yield a value of approximately 40% different from the experimental data (290 GPa compared to 208 GPa). The difference may result from the fact that hcp phase exists in extreme high pressure conditions, while this DFT calculation was performed at 0 K and 0 GPa. Also, the experimental evaluations of bulk modulus at high pressures generally come with large fluctuation error in measurements.

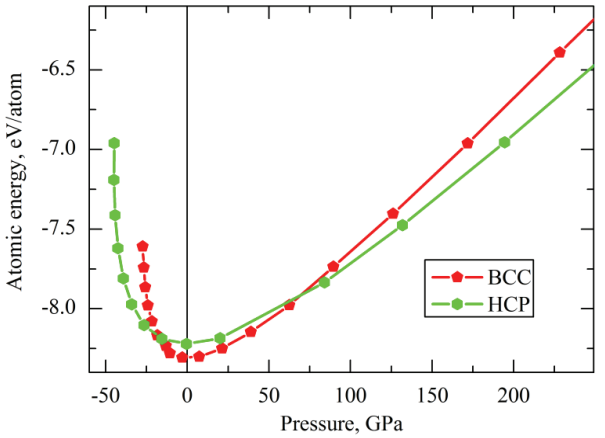

Figure 2: Variation of energy as a function of external pressure for bcc and hcp Fe

3.2 Elastic Constants: Second and Third Order

Calculations were made for SOEC and TOEC of bcc (Tab. 2) and hcp Fe (Tab. 3) at various points around zero pressure by fitting the strain energy using Eq. 6-10. Also, a set of elastic constants was reported for fcc phase at zero pressure in Tab.4. Utilizing the relationship of $B_0 = (C_{11}+C_{12})/3$ for cubic crystals, the bulk modulus, B_0, can be obtained from the values of C_{11} and C_{12}, in addition to the value derived from the EoS fit. From those two methods, the data still gave close agreements for bcc Fe (188.4 vs. 177.9 GPa) and fcc Fe (284.7 vs. 285.4 GPa). In addition, both bcc and fcc phases obey the lattice stability criteria for cubic crystals [Wang, Yip, Phillpot and Wolf (1993)], i.e., $B_0 > 0$, $G = C_{44} > 0$, $C_s = (C_{11}-C_{12})/2 > 0$, and all comply with the general rule: $B_0 > G > C_s$.

According to these calculations, most of the elastic constants (second and third-order) follow a linear dependence with respect to pressure (Fig.3 and Fig. 4 for

Table 2: Variation of bcc Fe elastic constants around zero pressure a: [Kellwege and Hellwege (1979)]; b: [Hughes and Kelly (1953)]; c: [Lew, Caspersen, Carter and Ortiz (2006)]

	This work								Expt.[a]	Expt.[b]	Theory [a,c]
V, A^3	11.09	11.21	11.27	11.34	11.35	11.36	11.43	11.51			11.46
P, GPa	4.56	2.32	1.29	0.22	0.00	-0.17	-1.20	-2.47			
SOEC, GPa											
C_{11}	308.41	286.26	275.75	265.13	263.04	261.37	252.27	241.59	243		271
C_{12}	163.09	158.60	155.93	152.07	151.14	150.41	146.35	139.74	138		145
C_{44}	119.12	111.55	107.93	104.11	103.34	102.74	99.14	94.73	122		101
TOEC, GPa											
C_{111}	-33526	-19798	-13273	-6367.1	-4971.5	-3907.4	2657.1	10676.3	-2829	-4820	-1644
C_{112}	-548.07	-618.00	-645.88	-667.44	-675.14	-679.73	-704.70	-749.85	-800	-700	-260
C_{123}	-861.23	-784.78	-774.70	-803.85	-806.29	-811.82	-862.68	-917.45	-607	2460	-300
C_{144}	-780.36	-744.25	-725.33	-702.94	-699.01	-695.79	-673.32	-646.87	–	-1580	-300
C_{155}	-643.07	-627.59	-618.72	-606.96	-606.69	-603.42	-591.38	-576.86	–	-1030	-260
C_{456}	-676.90	-663.47	-656.56	-648.66	-647.01	-645.72	-637.78	-627.15	–	275	-300

Table 3: Calculated elastic constant of fcc Fe at zero pressure, GPa

C_{11}	C_{12}	C_{44}	C_{111}	C_{112}	C_{123}	C_{144}	C_{166}	C_{456}
418.85	217.56	238.63	-4345.45	-926.34	-553.66	-297.33	-1077.43	-93.7

Table 4: Variation of hcp Fe elastic constants around zero pressure a: [Singh, Mao, Shu and Hemley (1998)]; b: [Soderlind, Moriarty and Wills (1996)]

	This work									Expt.[a]	Theory [b]
V, A^3/atom	9.94	10.06	10.09	10.11	10.16	10.18	10.19	10.21	10.26	–	9.70
P, GPa	7.12	3.26	2.52	1.78	0.34	0.00	-0.37	-1.07	-2.44	8.6	–
SOEC, GPa											
C_{11}	650.8	621.9	616.2	610.6	599.9	597.2	594.4	589.0	578.1	552(+/-65)	638
C_{12}	134.3	126.6	125.1	123.7	120.3	119.7	118.9	117.5	114.7	335(+/-60)	190
C_{13}	160.6	152.7	151.1	149.6	146.5	145.8	145.0	143.5	140.6	301(+/-45)	218
C_{33}	661.2	631.2	625.4	619.6	608.1	605.4	602.4	597.0	585.7	562(+/-80)	606
C_{44}	252.7	241.8	239.7	237.5	233.4	232.4	231.3	229.3	225.2	395(+/-30)	178
TOEC, GPa											
C_{111}	-44934.7	-24234.5	-20241.7	-16295.7	-8519.2	-6684.3	-4715.4	-957.0	6418.0		
C_{112}	-760.1	-728.5	-722.1	-716.3	-714.8	-712.6	-709.4	-703.8	-692.3		
C_{113}	-827.9	-793.1	-787.5	-781.7	-768.5	-764.2	-759.9	-754.5	-739.1		
C_{114}	-396.1	-379.0	-375.7	-372.4	-367.3	-365.9	-364.1	-361.2	-354.6		
C_{123}	-260.7	-248.7	-246.9	-244.5	-239.9	-238.0	-236.1	-234.7	-227.8		
C_{124}	176.5	168.6	166.9	164.0	164.8	164.4	163.7	162.7	159.3		
C_{133}	-698.9	-669.5	-662.7	-657.6	-653.5	-652.5	-650.8	-645.7	-640.8		
C_{134}	167.4	158.1	156.0	154.5	154.1	153.5	152.6	151.5	148.9		
C_{144}	-396.1	-379.0	-375.7	-372.4	-367.3	-365.9	-364.1	-361.2	-354.6		
C_{155}	-541.3	-531.0	-529.1	-528.5	-523.9	-522.9	-521.8	-519.9	-516.2		
C_{222}	-44934.7	-24234.5	-20241.7	-16295.7	-8519.2	-6684.3	-4715.4	-957.0	6418.0		
C_{333}	-45643.7	-24122.4	-19970.4	-15861.7	-7804.1	-5898.0	-3847.4	64.7	7746.7		
C_{344}	-1498.8	-1440.4	-1429.0	-1418.3	-1396.1	-1390.7	-1385.0	-1374.3	-1353.2		

Table 5: Calculated first pressure derivative of SOEC for bcc Fe (a: [Jephcoat, Mao and Bell (1986)])

	dC_{11}/dP	dC_{12}/dP	dC_{44}/dP	dB_0/dP
From values of TOEC	9.72	4.55	2.20	6.27
From plot of SOEC	9.70	4.35	3.57	6.13
From EOS	–	–	–	5.09
Expt.[a]	–	–	–	5.0

bcc; Fig. 5 and Fig. 6 for hcp Fe). C_{111}, C_{222} and C_{333} are nearly identical in hcp Fe. The values of TOEC in both phases (especially C_{111}) are very sensitive to pressure. For example, a variation of 0.1 GPa in external pressure may induce a change in bcc Fe C_{111} by 600 GPa.

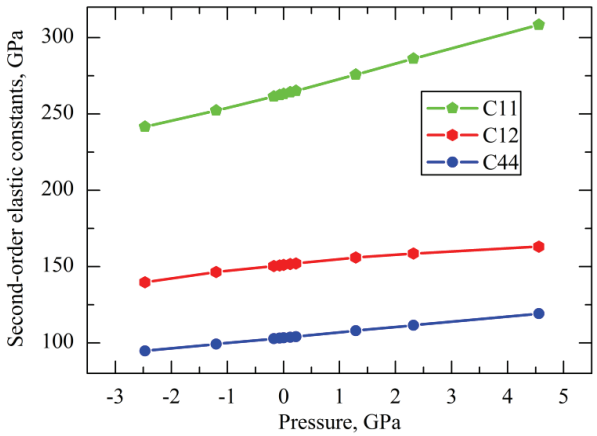

Figure 3: Variation of bcc Fe SOEC (GPa) as functions of pressure

The SOEC of bcc and hcp Fe positively vary with pressure, and this is a normal behavior for solids. The derivatives of SOEC can either be determined directly from the slope of SOEC lines or be calculated analytically, requiring the knowledge

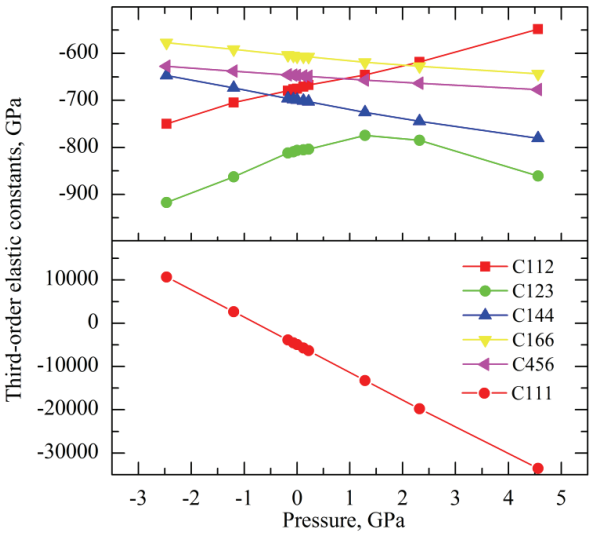

Figure 4: Variation of bcc Fe TOEC (GPa) as functions of pressure

of some TOEC.

$$\begin{aligned}
\frac{\partial C_{11}}{\partial P} &= -\frac{2C_{11}+2C_{12}+C_{111}+2C_{112}}{C_{11}+2C_{12}} \\
\frac{\partial C_{12}}{\partial P} &= -\frac{-C_{11}-C_{12}+2C_{112}+C_{123}}{C_{11}+2C_{12}} \\
\frac{\partial C_{44}}{\partial P} &= -\frac{C_{11}+2C_{12}+C_{44}+C_{144}+2C_{166}}{C_{11}+2C_{12}}
\end{aligned} \tag{11}$$

The results of dC_{11}/dP, dC_{12}/dP, and dB/dP are very consistent between two methods, while there is an observable difference in dC_{44}/dP (Tab. 5). The negative TOEC values of bcc and fcc Fe indicate that the increasing pressure will cause an increase in vibration frequencies. The behavior of bcc Fe under compression can be verified by studying the phonon dispersion curves in the next section.

3.3 Phonon dispersion of Iron polymorphs and Pressure dependence.

The calculated phonon dispersion curves of bcc, fcc, and hcp Fe are displayed in Fig. 7, in addition to the corresponding density of states (DOS) along the high symmetry lines of the Brillouin zone. Consistency is observed between our theoretical calculations and experimental data for bcc Fe [Hasegawa, Finnis and Pettifor (1987)], which were recorded at room temperature and zero pressure.

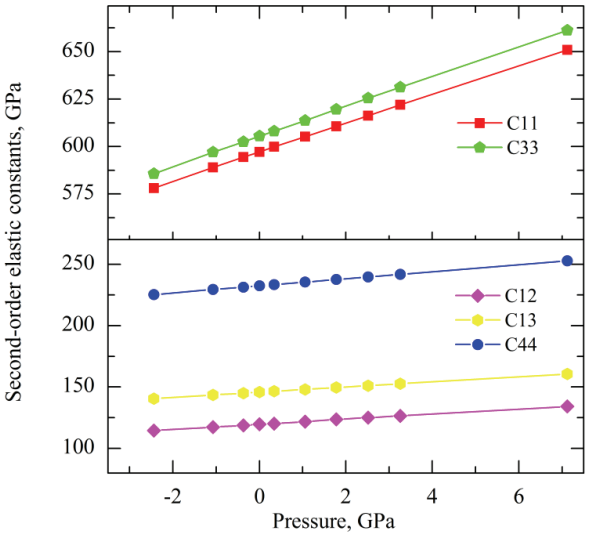

Figure 5: Variation of hcp Fe SOEC (GPa) as functions of pressure

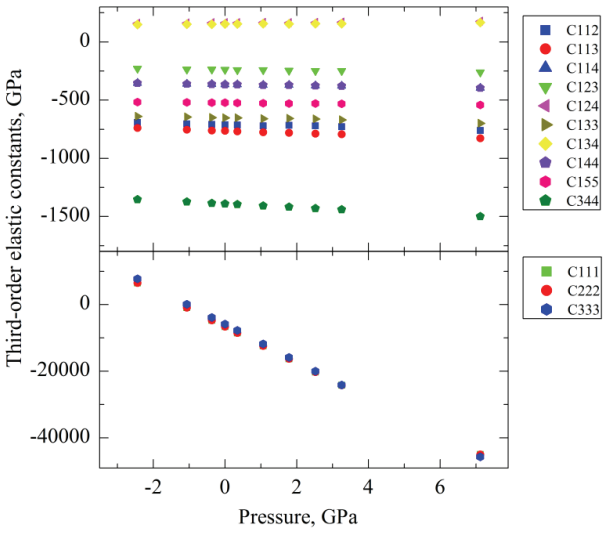

Figure 6: Variation of hcp Fe TOEC (GPa) as functions of pressure

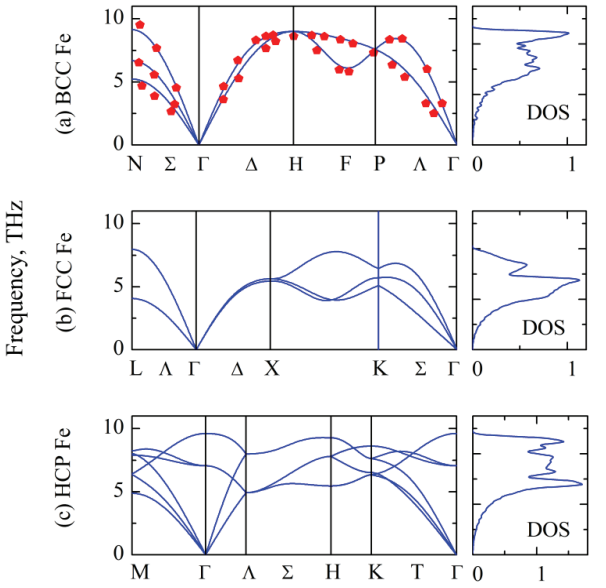

Figure 7: Phonon dispersion curves of bcc (a), fcc (b) and hcp (c) Fe at equilibrium. The red dots in BCC phonon are experimental data from [Hasegawa, Finni and Pettifor (1987)]

In order to assess the stability of Fe crystal at high pressures, the phonon spectra of bcc Fe is calculated under various compressions, as displayed in Fig. 8. Besides the expansion of the frequency range, negative frequency values were found for the optical branch after 200 GPa. This negative vibration frequency indicates instability in bcc Fe structure at high pressures. Similarly, the hcp Fe is studied at decreased pressures by expanding the unit cell volume beyond equilibrium volume (Fig. 9). After approximately a tensile pressure value of -40 GPa an negative frequency for the acoustic branch is recorded, i.e. indication of an unstable hcp phase. This observation implies that bcc Fe is more favorable at equilibrium, whereas hcp is dominant at extreme conditions.

4 Concluding Remarks

A complete set of SOEC and TOEC has been reported in three common phases of Fe: bcc, fcc and hcp. The calculations of their values at different pressures show a fairly linear dependence. Among the TOEC, C_{111} is most affected by the external stress. The study on phonon spectra confirms the instability of lattice vibration for

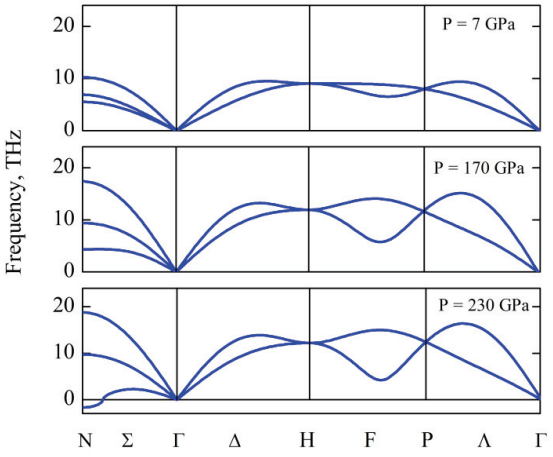

Figure 8: Phonon spectra of bcc Fe at increased pressure

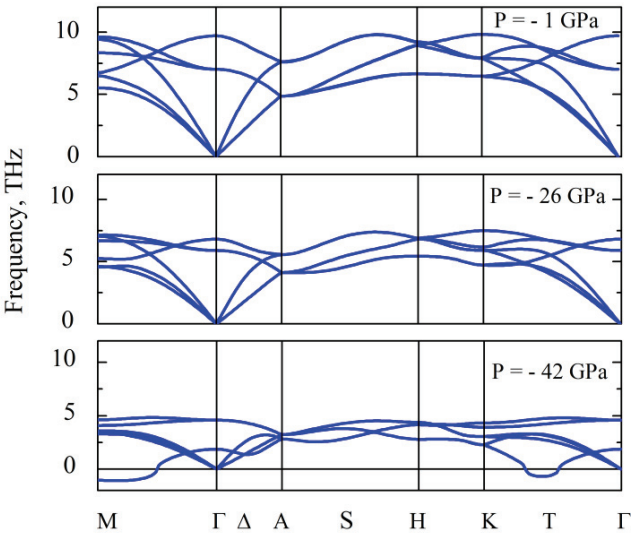

Figure 9: Phonon spectra of hcp Fe

bcc at high pressure and for hcp under tension.

Acknowledgement: The research here supported by NSF ITR_ASE: The authors would also like to thank the supercomputing center of Texas A&M University.

References

Bl ochl, P. E. (1994): Projector augmented-wave method. *Physical Review B 50*, 17953.

Brugger, K. (1964): Thermodynamic Definition of Higher Order Elastic Coefficients. *Physical Review A-General Physics 133*, 1611-&.

Bilge, M., Kart, H.H., Kart, S. O., and Çağın, T. (2009): B3-B1 Phase Transition and Pressure Dependence of the Elastic Properties of ZnS, *Materials Chemistry and Physics* 111, 559-64.

Çağın, T.; Pettitt, B. M. (1989): Elastic-Constants of Nickel - Variations with Respect to Temperature and Pressure. *Physical Review B 39*, 12484-12491.

Çağın, T.; Ray, J. R. (1988): 3rd-Order Elastic-Constants from Molecular-Dynamics - Theory and an Example Calculation. *Physical Review B 38*, 7940-7946.

Çağın, T., Karasawa, N., Dasgupta, S. D., and Goddard, W. A. (1992): Thermodynamic and Elastic Properties of Polyethylene at Elevated Temperatures, in *Computational Methods in Materials Science*, Materials Research Society Symposium Proceedings 278: 61-66.

Çağın, T. (1993): Mechanical Response of High Performance Polymers, in *Materials Theory and Modeling*, Materials Research Society Symposium Proceedings 291: 321-324.

Çağın, T., Kimura, K., Qi, Y., Ikeda, H., Johnson, W. L. and Goddard, W. A. (1999): Calculation of mechanical, thermodynamic and transport properties of metallic glass formers in *Bulk Metallic Glasses*, Materials Research Society Symposium Proceedings 554: 43-48.

Chakrabarty, A. and Çağın, T. (2008): Modeling Mechanical and Thermal Properties of Nanotube Based Nanostructures , *CMC: Computers, Materials and Continua* 7, 167-189.

Fritz, I. J.; Graham, R. A. (1974): Second-Order Elastic-Constants of High-Purity Vitreous Silica. *Journal of Applied Physics 45*, 4124-4125.

Fumi, F. G. (1951): 3rd-Order Elastic Coefficients of Crystals. *Physical Review 83*, 1274-1275.

Fumi, F. G. (1952): 3rd-Order Elastic Coefficients in Trigonal and Hexagonal Crystals. *Physical Review 86*, 561-561.

Graham, R. A. (1972): Determination of Third-Order and Fourth-Order Longitudinal Elastic-Constants by Shock Compression Techniques - Application to Sapphire and Fused Quartz. *Journal of the Acoustical Society of America 51*, 1576-&.

Hasegawa, H.; Finnis, M. W.; Pettifor, D. G. (1987): Phonon Softening in Ferromagnetic Bcc Iron. *Journal of Physics F-Metal Physics 17*, 2049-2055.

Hiki, Y. (1981): Higher-Order Elastic-Constants of Solids. *Annual Review of Materials Science 11*, 51-73.

Hughes, D. S.; Kelly, J. L. (1953): 2nd-Order Elastic Deformation of Solids. *Physical Review 92*, 1145-1149.

Hull, D.; Bacon, D. J. (2001): *Introduction to dislocations*. Oxford [England] ; Boston: Butterworth-Heinemann.

Jephcoat, A.; Olson, P. (1987): Is the Inner Core of the Earth Pure Iron. *Nature 325*, 332-335.

Jephcoat, A. P.; Mao, H. K.; Bell, P. M. (1986): Static Compression of Iron to 78-Gpa with Rare-Gas Solids as Pressure-Transmitting Media. *Journal of Geophysical Research-Solid Earth and Planets 91*, 4677-4684.

Jiang, D. E.; Carter, E. A. (2003): Carbon dissolution and diffusion in ferrite and austenite from first principles. *Physical Review B 67*, 214103.

Johal, A. S.; Dunstan, D. J. (2006): Reappraisal of experimental values of third-order elastic constants of some cubic semiconductors and metals. *Physical Review B 73*, .

Kalay, M., Kart, H. H., Kart, S. O. and Çağın, T. (2009): Structural parameters, elastic constants and transition pressures of ZnO from first-principle calculations, *J. Alloy. Comp.*484, 431-438

Kart, S. O., Uludogan, M., Karaman, I. and Çağın, T. (2008): DFT Studies on Structure, Mechanics and Phase Behavior of Magnetic Shape Memory Alloys: Ni2MnGa *Phys. Stat. Sol.* (a) 205, 1026-35

Kellwege, K.-H.; Hellwege, A. M. (1979): Landolt-Bornstein. Numerical Data and Functional Relationships in Science and Technology New Series. Group III: Crystal and Solid State Physics. Volume 11 (Revised and Extended Edition of Volumes III/1 and III/2). Elastic, Piezoelectric, Pyroelectric, Piezooptic, Electrooptic Constants, and Nonlinear Dielectric Susceptibilities of Crystals. M.M. Choy, W.R. Cook, R.F.S. Hearmon, J. Jaffe, J. Jerphagnon, S.K. Kurtz, S.T. Liu, and D.F. Nelson.

Kohn, W.; Sham, L. J. (1965): Self-Consistent Equations Including Exchange and Correlation Effects. *Physical Review 140*, 1133-&.

Kresse, G.; Furthmuller, J. (1996): Efficient iterative schemes for ab initio total-

energy calculations using a plane-wave basis set. *Physical Review B 54*, 11169-11186.

Laio, A., Bernard, S., Chiarotti, G. L., Scandolo, S. and Tosatti, E. (2000): Physics of iron at Earth's core conditions. *Science 287*, 1027-1030.

Lew, A., Caspersen, K., Carter, E. A. and Ortiz, M. (2006): Quantum mechanics based multiscale modeling of stress-induced phase transformations in iron. *Journal of the Mechanics and Physics of Solids 54*, 1276-1303.

Li, J. H., Liang, S. H.,Guo, H. B. and Liu, B. X. (2005): Four-parameter equation of state of solids. *Applied Physics Letters 87 (19): 194111*-194113.

Lopuszynski, M. and Majewski, J. A. (2007): Ab initio calculations of third-order elastic constants and related properties for selected semiconductors. *Physical Review B 76*, -.

Mehl, M. J.;Osburn, J. E.;Papaconstantopoulos, D. A.; Klein, B. M. (1990): Structural-Properties of Ordered High-Melting-Temperature Intermetallic Alloys from 1st-Principles Total-Energy Calculations. *Physical Review B 41*, 10311-10323.

Monkhorst, H. J.; Pack, J. D. (1976): Special Points for Brillouin-Zone Integrations. *Physical Review B 13*, 5188-5192.

Murnaghan, F. D. (1967): *Finite deformation of an elastic solid*. New York,: Dover Publications.

Nakagawa, Y., Yamanouc, K. and Shibayam, K. (1973): Third-Order Elastic-Constants of Lithium-Niobate. *Journal of Applied Physics 44*, 3969-3974.

Nielsen, O. H. (1986): Optical Phonons and Elasticity of Diamond at Megabar Stresses. *Physical Review B 34*, 5808-5819.

Nye, J. F. (1957): *Physical properties of crystals, their representation by tensors and matrices*. Oxford,: Clarendon Press.

Ojeda,O. U. and Çağın, T. (2010): Multiscale modeling of crystalline energetic materials . *CMC: Computers, Materials and Continua,* this issue.

Perdew, J. P.;Burke, K.; Ernzerhof, M. (1996): Generalized Gradient Approximation Made Simple. *Physical Review Letters 77*, 3865.

Sevik, C. and Çağın, T. (2009): Structure and electronic properties of CeO_2, ThO_2 and their alloys, *Physical Review B. 80*, 014108

Sha, X. W.; Cohen, R. E. (2006): Lattice dynamics and thermodynamics of bcc iron under pressure: First-principles linear response study. *Physical Review B 73*, 104303.

Singh, A. K.; Mao, H. K.; Shu, J. F.; Hemley, R. J. (1998): Estimation of single-crystal elastic moduli from polycrystalline X-ray diffraction at high pressure: Ap-

plication to FeO and iron. *Physical Review Letters 80*, 2157-2160.

Soderlind, P.; Moriarty, J. A.; Wills, J. M. (1996): First-principles theory of iron up to earth-core pressures: Structural, vibrational, and elastic properties. *Physical Review B 53*, 14063-14072.

Song, X. D.; Richards, P. G. (1996): Seismological evidence for differential rotation of the Earth's inner core. *Nature 382*, 221-224.

Steinle-Neumann, G.; Stixrude, L.; Cohen, R. E.; Gulseren, O. (2001): Elasticity of iron at the temperature of the Earth's inner core. *Nature 413*, 57-60.

Stixrude, L.; Cohen, R. E. (1995): Constraints on the Crystalline-Structure of the Inner-Core - Mechanical Instability of Bcc Iron at High-Pressure. *Geophysical Research Letters 22*, 125-128.

Stixrude, L.; Cohen, R. E. (1995): High-Pressure Elasticity of Iron and Anisotropy of Earths Inner-Core. *Science 267*, 1972-1975.

Uludogan, M., Çağın, T. and Goddard W.A. (2006): First Principles Approach to $BaTiO_3$ Turk. J. Phys. 30, 277-285.

Uludogan, M., Guarin, D.P., Gomez, Z. E., Çağın, T. and Goddard W.A. (2008): DFT studies on ferroelectric ceramics and their alloys *CMES: Computer Modeling in Engineering and Sciences*, Vol. 24, 215-38.

Vinet, P.; Ferrante, J.; Rose, J. H.; Smith, J. R. (1987): Compressibility of Solids. *Journal of Geophysical Research-Solid Earth and Planets 92*, 9319-9325.

Wallace, D. C. (1972): *Thermodynamics of crystals*. New York,: Wiley.

Wang, J. H.; Yip, S.; Phillpot, S. R.; Wolf, D. (1993): Crystal Instabilities at Finite Strain. *Physical Review Letters 71*, 4182-4185.

Yoo, C. S.; Akella, J.; Campbell, A. J.; Mao, H. K.; Hemley, R. J. (1995): Phase-Diagram of Iron by in-Situ X-Ray-Diffraction - Implications for Earth Core. *Science 270*, 1473-1475.

Zhao, J. J.; Winey, J. M.; Gupta, Y. M. (2007): First-principles calculations of second- and third-order elastic constants for single crystals of arbitrary symmetry. *Physical Review B 75*, 094105.